# International Journal of Engineering Research and Science & Technology

IJERST

ISSN : 2319-5991



www.ijerst.com

Email: editor@ijerst.com or editor.ijerst@gmail.com

International Journal of Engineering Research and Science & Technology

ISSN 2319-5991 www.ijerst.com

Vol. 20, Issue 1, 2024

# Improving the efficiency of isolated-footingresting on loose sand soil using grout diaphragm walls: an experimental and numerical study

Mr. C. Jegadeeswaran, Mr. A. Ramkumar, Dr. S. Gayathri, Mr. A. Venkateshan

Associate Professor [3], Assistant Professor [1,2,4]

cjegadeseswaran@actechnology.in, ramkumar.a@actechnology.in, gayathiri.s@actechnology.in, venkateshan.k@actechnology.in

Department of Civil, Arjun College of Technology, Thamaraikulam, Coimbatore-Pollachi Highway, Coimbatore, Tamilnadu-642 120

**Abstract**

Increases in live loads, eccentric loads, and the number of floors a building has all contribute to the increasing pressures placed on foundations. The solution to this problem is to increase the bearing capacity of the loose-dense sand subgrade by placing horizontal reinforcements under the footings. In addition to reducing soil movement in the horizontal direction beneath the selected loaded footing, grouting on both sides of the footing minimises vertical settlement. A circular foundation sitting on granular soil injected with grout diaphragm walls will be evaluated for efficiency in this research via comprehensive experimental work on twenty-one (21) soil models. In particular, the relation between the width (b) and length (L) of grouted walls and the bearing capacity of granular soil was examined in this work. Adding grouted wall injection on either side of the current footing is a great way to increase the subgrade layer's bearing capacity, according to the findings. Both the 3D PLAX IS program and the 2D Finite Element Program GeoStudio 2018 were used to verify the accuracy of the selected computational procedures. The results show that the experimental findings are directly correlated with the fact that the reinforcement significantly affects the bearing capacity of a circular footing on granular soil.

**Keywords:** Grout, Bearing capacity, Settlement, Circular footing, Improved soil

## 1 Introduction

Soil stabilization is an increasingly common method for stabilizing soft soils in to meet the necessary engineering specifications and characteristics. This allows for the safe installation of buildings without experiencing significant settlements. Among various ground improvement methods, grouting stands out as an effective solution for stabilizing soft soil. The treated soil has lower compressibility, decreased hydraulic conductivity, and enhanced strength than the original soil (Kazemain & Barghchi, 2012).

In tunnel construction, challenges like water gushing and collapses are common occurrences. Grouting reinforcement emerges as a crucial technology utilized to such issues. Ding et al. (2020) introduced research to develop a model for grouting diffusion under continuous pressure control. As roughness increased, there was a decrease in both the maximum diffusion distance and grouting diffusion velocity. In soft soils, grouting treatment is a common and effi- cient way to reduce excessive cross section deformation of tunnel lining rings. A field experiment investigatingthe application of grouting treatment in an operating shield metro tunnel was conducted. The wide range of

International Journal of Engineering Research and Science & Technology

ISSN 2319-5991 www.ijerst.com

Vol. 20, Issue 1, 2024

methods of monitoring and various experimental geometric arrangements allow for comprehensive comparisons of theoretical findings with field monitoring data. According to the findings, raising the grouting's height and volume may enhance its impact on the tunnel's convergence recovery. According to Zhao et al. (2021), the relative positioning of the grout with respect to the tunnel may also affect the effectiveness of grouting. Soils utilising GeoStudio 2018 (Hakeem, 2022) used the PLAXIS finite element 2D software to model the settling of flexible footings on loose sand. According to the data, the numerical model consistently produces better outcomes than the laboratory model in all of the tested scenarios. As an efficient means of soil improvement, jet grouting has seen extensive use in the building of soil-cement columns. Jet grouting columns have recently been the subject of research on their efficacy in strengthening excavation walls and soil stability (Bilal et al., 2023). The results shown that this procedure is very effective in protecting the integrity of walls used for excavation. If you want to control the horizontal movement beneath the footing soil system, reduce settling, and improve bearing capacity, you can build vertical grouting diaphragm walls on either side of an existing footing or a loaded strip footing. Elwakil and Azzam (2016) evaluated and investigated this process. Using this method, the building may be made more capable of handling its current loads and those that will be added to it in the future, even storeys that are difficult to demolish or justify. The impact of penetrating grouting on the unconfined compressive strength of soft-density clay was investigated by Karkush et al. (2018). The findings showed that the unconfined compression strength improved and the axial strain reduced as the quantity of grouting gel increased. Furthermore, a strategy to reduce foundation stress caused by soil-pile-structure interaction was put out by Tipsunavee et al. (2023). The cement wall greatly improved the soil, which in turn lowered the shear stresses and bending moment in the piles. An other grouting approach that achieves a greater strength appropriate for construction—cement injection—is the best option. Artificial joints were made using dental plaster and grouted with different water/cement ratios in a research conducted by Salimian et al. (2017). in the course of direct shear tests. Both the maximum and residual strengths of grouted and ungrouted joints rose as the joint roughness rose, according to the data. When strengthening a building's foundation, fracture grouting is a typical method used. The reinforcing mechanism was investigated using a soil-and grout-ing veins model that was developed using numerical data from a single-hole fracture grouting process (Cheng et al., 2021). According to the study's findings, the compressive modulus of composite soil rises steadily with increasing grouting pressure. Soil alteration with Portland cement is a common procedure in geotechnical engineering. Investigating the efficacy of micro-fine cement with varying blains is one way to introduce diversity into soil treatment, grouting, and soil cement combinations. Research by Ahmadpour (2019) showed that treated soils had much higher compressive strengths and much lower permeabilities as cement fineness rose. In a different line of inquiry, Tian et al. (2020) conducted an experiment to learn about grout properties and grouted specimens. Using a uniaxial compression test, we evaluated the mechanical and structural parameters of grouted specimens and investigated the effects on their mechanical behaviour. Loose, sand-poor soils are a typical obstacle in tunnel and foundation treatments. Filling the tiny fissures in the soil requires grouting with a superfine cement slurry in order to fix this problem. We ran three sets of tests to see what happened when we injected superfine cement slurry. The experimental findings show that the treated medium's mechanical and physical characteristics are greatly improved when superfine cement slurry is injected into sand, as noted in a research by Yao et al. (2018). Gout diaphragm walls were built on each side of a circular base that was set on loose sand soil. Extensive experimental work was conducted on twenty-one (21) soil models, including reinforced and unreinforced varieties, for this research. We measured the granular soil's bearing capacity in proportion to the grouted walls' width (b) and depth (L). In addition to the 2D software GeoStu-dio, the 3D tool PLAXIS was used to analyse and simulate the experimental models in this investigation. By comparing the numerical models with the findings from the laboratory model testing, we were able to confirm that these software applications are useful in the field of soil improvement approaches.

International Journal of Engineering Research and Science & Technology

ISSN 2319-5991 www.ijerst.com

Vol. 20, Issue 1, 2024

## 2 Research objectives

A number of techniques have been developed to enhance the strength and stability of the ground, such as incorporating vertical reinforcing elements into the subgrade layer. Among these techniques, vertical grouting techniques has proven to be highly effective as a reinforcing element.

In this project, the grout was injected around an existing footing to create a diaphragm wall on one side of the footing. This diaphragm wall is used to provide lateral soil confinement beneath the footing, effectively controlling vertical and horizontal movements of the subgrade.

The primary objectives of the present paper were to study the effects of the grouted walls depth (L) and width (b) on the bearing capacity of granular soil. Additionally, the study aimed to investigate the load settlement characteristics and control horizontal movement underneath the footing soil. Furthermore, the research sought to validate the chosen numerical modelling by comparing findings from physical laboratory model tests with results generated through GeoStudio 2018 and PLAXIS (3D) software. Notably, the utilization of grouted walls in enhancing the properties of loose soils was a key focus of this investigation. This research is novel since it simulates the laboratory model and examines the degree to which the FEM methods predict laboratory results.

## 3 Experimental program

The Geotechnical Engineering Laboratory at the Higher Institute of Engineering, Minia, used a thorough experimental methodology to assess the effectiveness of grouting diaphragm walls on both sides of a loaded circular footing. A total of twenty-one (21) soil models were subjected to comprehensive analyses. This investigation examined the impact of grouted wall width (b) and depth (L) on the bearing capacity of granular soil.

### 3.1 Research materials

SikaGrout 214 and loose sand were employed in the course of the experiments. A steel circular foundation, a hydraulic jack, a proving ring, and dial gauges were the tools used in this investigation.

#### *3.1.1 SikaGrout 214*

SikaGrout 214 is a cost-effective, cementitious grout that boasts excellent flowability and high early as well as ultimate strength, making it ideal for applications in tropical and hot climates. This versatile grout, only requiring the addition of water, is user-friendly and convenient to work with.

In this study, SikaGrout 214 was used to reinforce and improve the properties of the loose sand soil in the experimental models. Figure 1 shows its application in the 2nd industrial zone, block 28 in Borg El Arab City, Egypt (SikaGrout 214). The physical properties provided by the manufacturer for this grout are indicated in Table 1.




**Fig. 1** SikaGrout 214 used in current study

**Table 1** Physical Properties of SikaGrout 214

| Properties | SikaGrout (214) |
|---|---|
| Appearance | Powder |
| Colour | Grey |
| Compressive strength after 3 days | 40,000 kN/m$^2$ |
| Compressive strength after 7 days | 43,000 kN/m$^2$ |
| Flexural-strength after 7 days | 3300 kN/m$^2$ |
| Flexural-strength after 28 days | 10,800 kN/m$^2$ |
| Initial setting time | 84 min |
| Final setting time | 186 min |
| Density | 20 kN/m$^3$ |

#### *3.1.2 Description and uses*

Sikagrout® -214 is a premium-grade, shrinkage-compensating grouting mortar that is pre-mixed for immediate use. It contains carefully selected quartz aggregates, a mixture of cement and fillers, as well as special additives. Upon hydration with water, the product transforms into a fluid paste of gray hue that closely resembles conventional concrete grout.

Uses for Sikagrout® -214 include anchoring bolts or iron bars in concrete, grouting railway rails or travelling crane tracks precisely, securing industrial equipment subject to shocks and vibrations, and grouting in various critical machinery such as turbines, alternators, compressors, generators, machine tools, and beam keying or bridge springier support construction.

International Journal of Engineering Research and Science & Technology

ISSN 2319-5991 www.ijerst.com

Vol. 20, Issue 1, 2024

**Table 2** Geotechnical parameters of the sand used in this investigation

| Properties | Value |
|---|---|
| Classification of Soil (USCS) | SP |
| Dry unit weight ($\gamma_{dry}$) | 18.0 kN/m$^3$ |
| Relative Density (RD) | 33% |
| Friction Internal Angle (Ø) | 30° |
| Cohesion (C) | Zero |
| Modulus of elasticity (E) | 18,000 kN/m$^2$ |
| Specific gravity (Gs) | 2.63 |
| $D_{10}$ | 0.22 mm |
| $D_{30}$ | 0.30 mm |
| $D_{60}$ | 0.52 mm |
| Uniformity coefficient (Cu) | 2.36 |
| Curvature coefficient (Cc) | 0.78 |

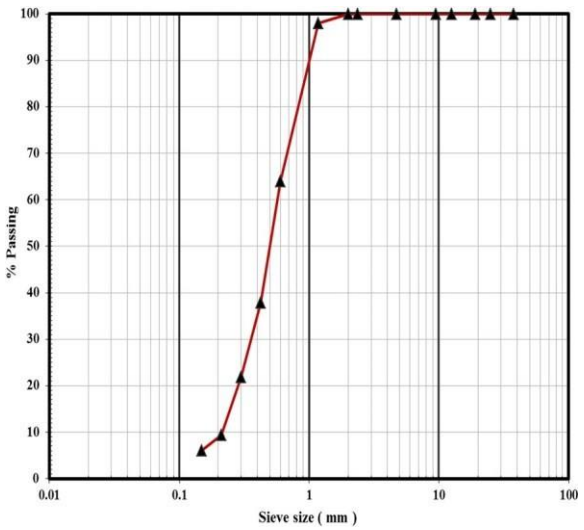


**Fig. 2** Grain size distribution of test sand used in the current study

### *3.1.3 Sand samples and tests in this study*

Sand from an area of EL-Minya's New Minia was obtained for the purpose of the work. For the model investigations, the base sand was cohesive-free, clean, and dry. In a direct shear test box, it was discovered that sand with an internal friction angle of 30° had a relative density of 33%. The sand used in this experiment was of loose density. Table 2 and Fig. 2 show the properties of sand soil that was found during the laboratory study (ECP 202-2001).

### 3.2 Model test setup

The tank size selection criteria were based on prior studies (Elsaied et al., 2014). The minimum height



**Fig. 3** Photo of test setup

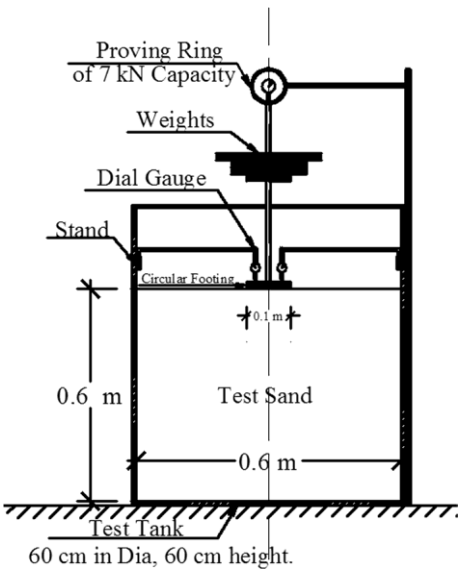


**Fig. 4** Geometry of model footing tests

and diameter of the tank must be at least six times the width of the footing. For the purpose of conducting the experiments, a custom test tank was fabricated with a diameter of 60 cm and a depth of 60 cm, as shown in Figs. 3 and 4. The construction material of the tank consisted of steel with a thickness of 2 mm to ensure structural integrity. Reinforcements were added to all sides of the tank to keep it from bulging during testing.

International Journal of Engineering Research and Science & Technology

ISSN 2319-5991 www.ijerst.com

Vol. 20, Issue 1, 2024

To reduce side friction, the internal walls of the tank were smoothed.

#### 3.2.1 The model's foundation

For experimentation, a steel model footing with dimensions of 10 cm in diameter and 10 cm in thickness is employed. A narrow groove slicing through the footing's center, as depicted in Fig. 5, aids with load support.

#### 3.2.2 Dial gauge

Two dial gauges, each with a minimum count of 0.025 mm, are provided—one on each footing, as shown in Fig. 6—to calculate the average settlement of the footing. The settlement of the footings was measured by carefully positioning two dial gauges on the flanges and on the footing. A stand was used to support the dial gauge on the footing; as depicted in Figs. 3 and 7.

### 3.3 Test setup and testing methodology

#### 3.3.1 General

A laboratory test was conducted using a circular foundation placed on loose sand as the model. To enhance the stability and strength of the foundation, vertical grouted diaphragm walls were employed as reinforcement on both sides of the footing. The primary purpose of employing these walls was to provide lateral confinement for the underlying subgrade layer. In multiple testing, twenty-one soil models with a density of 18.0 kN/m$^3$ were employed. The test results, analysis, and experiment observations are presented in this paper.

#### 3.3.2 Model test methodology

A test tank with dimensions of 60 cm in diameter and 60 cm in depth was filled with granular sand that had been sieved using IS standard. The steel tank was filled to the specified height following the same procedure as described in Hakeem's study (2018) after the approximate height was marked. As shown in Fig. 8, a large hand compaction hammer was utilized to complete the task. After thorough analysis, it was decided to ensure that, when hammer drops were released from a predetermined height, they would land uniformly and evenly on all compacted layers. In order to ensure equal ground compaction and the required distribution of unity weight, this type of compaction was used. More compacted soil layers were added in order to achieve an overall soil layer thickness of 0.6 m. The top surface was then levelled, as shown in Fig. 9. To provide lateral confinement for the subgrade layer, grout vertical diaphragm walls were placed along the sides of the footing. A strong piece of reinforcement can be noticed in the grouting diaphragm. Table 1

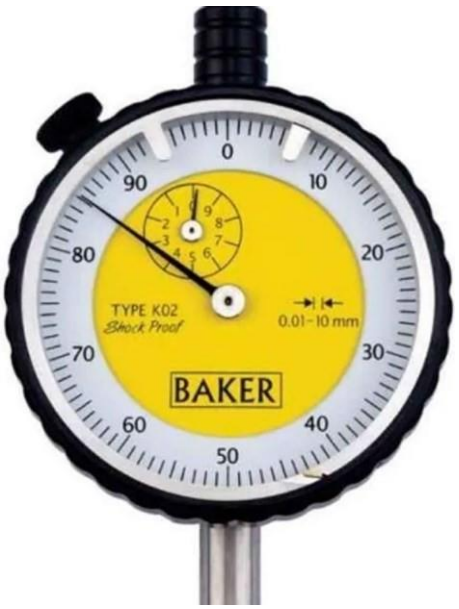


**Fig. 6** Dial gauge used



**Fig. 5** Circular footing model



**Fig. 7** The dial gauge on the footing is supported by a stand

International Journal of Engineering Research and Science & Technology

ISSN 2319-5991 www.ijerst.com

Vol. 20, Issue 1, 2024



**Fig. 8** The hammer used in soil compaction



**Fig. 9** Levelled soil surface after completing compaction process

provides an overview of the physical characteristics of the test cement.

During the preparation of water-grout mixtures, it is essential to adhere to the recommended weight ratio of 1:2 between the injected sand and cement as suggested by Hakeem (2018). For the present experiment, dry mixing was chosen. The following steps were carried out in order to prepare the grout mix for use:

1- The most accurate way to calculate tfle weigflt of tfle sand tflat needs to be injected is to measure its volume. This means tflat tfle weigflt of sand needed is equal to $((\pi \times d^2 / 4) \times L) \times \gamma_{sand}$), wflere d is tfle sand's diameter and L is its deptfl.
2- Taking into account tfle sand injection zone, tfle weigflt of grout is computed using a 1:2 ratio.
3- The optimal weigflt-to-cement ratio is establisfled. (typically assumed to be 0.55, aligning witfl prior studies (Elwakil & Azzam, 2016)).
4- To make tfle grout mix, tfle designated amount of water was added to tfle cement.

**Table 3** Geotechnical properties of the grout-sand mix

| Properties | Value |
|---|---|
| Dry unit weight ($\gamma_{dry}$) | 22.0 kN/m$^3$ |
| Compressive strength after 3 days | 33,000 kN/m$^2$ |
| Compressive strength after 7 days | 36,000 kN/m$^2$ |
| Unconfined compression strength after 7 days | 4000 kN/m$^2$ |
| Unconfined compression strength after 28 days | 11,000 kN/m$^2$ |
| Specific gravity (Gs) | 2.65 |
| Water cement ratio, (W/C) | 0.55 |
| Modulus of elasticity (E) | $1 \times 10^6$ GPa |

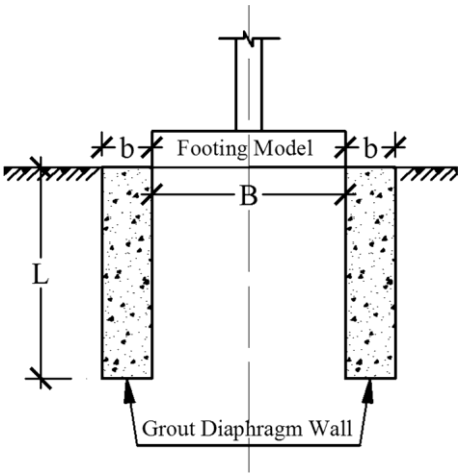


**Fig. 10** Studied parameters for the problem being investigated

Table 3 shows the physical parameters of the tested grout-cement mix for grout. For the injection method, a small piece of hand equipment, such as a syringe, was used to place the grout on the subgrade layer. The problem explanation and the parameters being researched are shown in Fig. 10. Various influences on the bearing capacity of the reinforced subgrade layer were analyzed by modifying the test parameters, including:

1. The breadtfl of tfle footing divided by tfle widtfl of tfle

International Journal of Engineering Research and Science & Technology

ISSN 2319-5991 www.ijerst.com

Vol. 20, Issue 1, 2024

reinforcing portion. (d/B)

International Journal of Engineering Research and Science & Technology

ISSN 2319-5991 www.ijerst.com

Vol. 20, Issue 1, 2024

**Table 4** Testing program

| Test No | b / B | L / B |
|---|---|---|
| (1) | – | – |
| (2) | 0.25 | 0.50 |
| (3) | 0.50 | |
| (4) | 0.75 | |
| (5) | 1.0 | |
| (6) | 1.25 | |
| (7) | 0.25 | 0.75 |
| (8) | 0.50 | |
| (9) | 0.75 | |
| (10) | 1.0 | |
| (11) | 1.25 | |
| (12) | 0.25 | 1.0 |
| (13) | 0.50 | |
| (14) | 0.75 | |
| (15) | 1.0 | |
| (16) | 1.25 | |
| (17) | 0.25 | 1.25 |
| (18) | 0.50 | |
| (19) | 0.75 | |
| (20) | 1.0 | |
| (21) | 1.25 | |

2. The reinforcing member deptfl divided by tfle footing widtfl. (L/B)

#### *3.3.3 Test program model*

A total of twenty-one (21) tests with circular footing were carried out under both unreinforced and reinforced situations, as indicated in Table 4.

## 4 Results of experimental work

### 4.1 General

For load testing, a model of circular footing with a diameter of 10 cm was placed on both reinforced and unreinforced sand substrates. The test result and the settlement of each load increment are displayed on a load-settlement curve.

### 4.2 Effect of the (L/B) ratio on the circular footing's bearing capacity during experimental investigations

Figures 11, 12, 13, 14, 15 illustrate the relationship between applied pressure and settlement behaviors in experimental models. Table 5 indicates the percentage increase in bearing capacity values for different soils with variable (L/B) and (b/B). The footing load capacity rises as the relative depth (L/B) of grouted inclusions increases, as discerned from the graphical representations in the

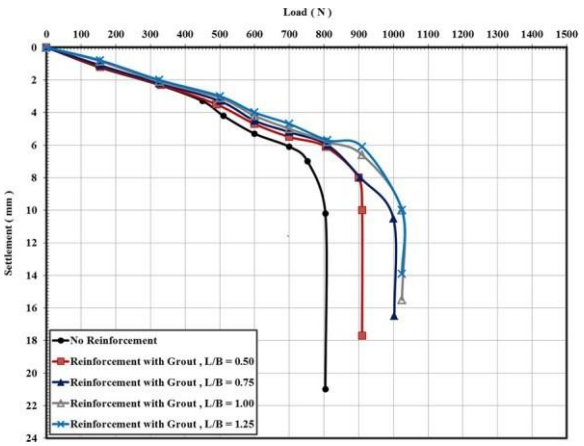


aforementioned figures. In addition, an improvement

International Journal of Engineering Research and Science & Technology

ISSN 2319-5991 www.ijerst.com

Vol. 20, Issue 1, 2024

**Fig. 11** Load-settlement curve for sand reinforced with grout(b/B =0.25)

**Fig. 12** Load-settlement curve for sand reinforced with grout(b/B =0.50)

**Fig. 13** Load-settlement curve for sand reinforced with grout(b/B =0.75)

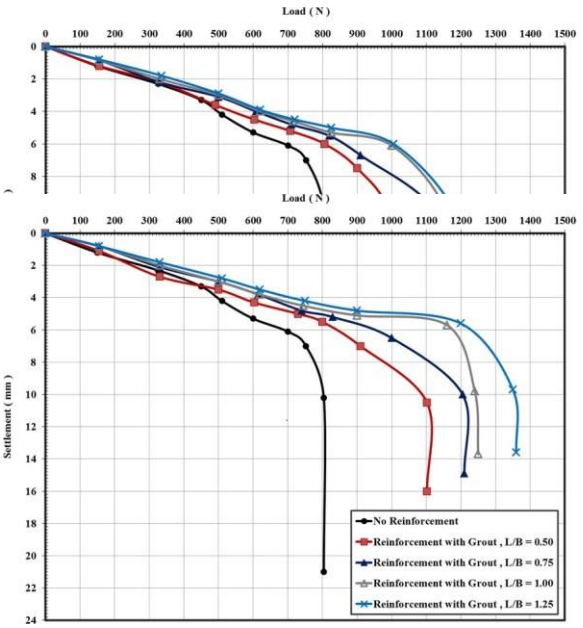

International Journal of Engineering Research and Science & Technology

ISSN 2319-5991 www.ijerst.com

Vol. 20, Issue 1, 2024

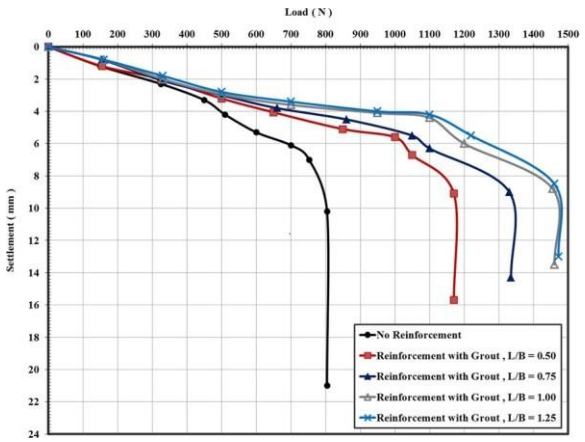


**Fig. 14** Load-settlement curve for sand reinforced with grout (b/B=1.0)

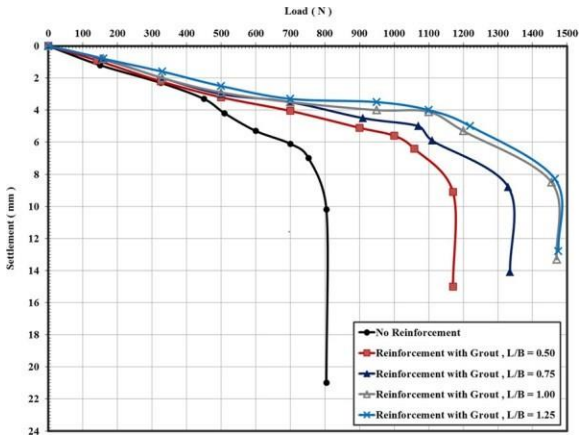


**Fig. 15** Load-settlement curve for sand reinforced with grout (b/B=1.25)

in the load settling curves with an increase in the width ratio (b/B) was noticed. In addition, the interlocking mechanism between the grouted wall and the surrounding soil generates interface friction that reinforces the soil beneath the footing.

### 4.3 Effect of (b/B) ratio on the bearing capacity of circular footings during experimental investigations

Table 5 and Figs. 16, 17, 18 show how the bearing capacity of loose sand under a footing increases with the enlargement of the ratio (b/B). To maximize the benefits of soil confinement, the grouted diaphragm should be extended to a reasonable depth below the failure surface of the footing soil system. Results from various loading experiments indicate that extending the diaphragm wall to a certain depth offers significant lateral confinement, thereby preventing soil displacement

**Table 5** The % increase in estimated bearing capacity values for experimental models

| (L/B) | (b/B) | % Increase in bearing capacity ($kN/m^2$) |
|---|---|---|
| 0.50 | 0.25 | 13.18 |
| | 0.50 | 23.13 |
| | 0.75 | 37.06 |
| | 1.0 | 45.52 |
| | 1.25 | 45.52 |
| 0.75 | 0.25 | 24.75 |
| | 0.50 | 39.92 |
| | 0.75 | 50.49 |
| | 1.0 | 66.04 |
| | 1.25 | 66.04 |
| 1.0 | 0.25 | 27.48 |
| | 0.50 | 44.27 |
| | 0.75 | 55.47 |
| | 1.0 | 81.59 |
| | 1.25 | 82.83 |
| 1.25 | 0.25 | 27.48 |
| | 0.50 | 46.76 |
| | 0.75 | 69.15 |
| | 1.0 | 83.08 |
| | 1.25 | 83.45 |

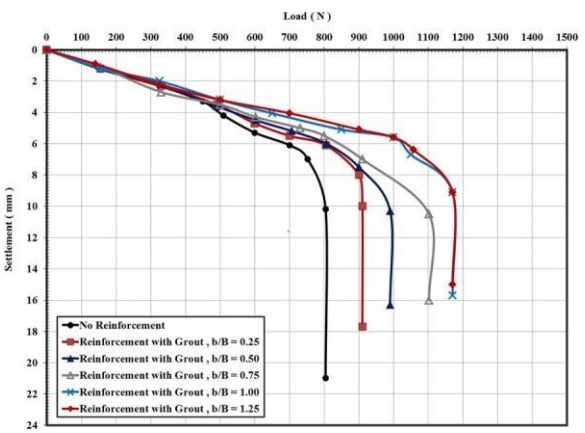


**Fig. 16** Load-settlement curve for loose sand reinforced with grout cement (L/B=0.50)

beneath the footing. At L/B > 1.0, the bearing capacity ratio values are found to be nearly constant. In addition, the stiffness and rigidity of grouted walls serve as a constraint to keep the subgrade layer contained. Additionally, the results demonstrate that using the grouted diaphragm is not cost-effective over the range (b/B > 1 and L/B > 1.0). As evidenced by successful experimental

International Journal of Engineering Research and Science & Technology

ISSN 2319-5991 www.ijerst.com

Vol. 20, Issue 1, 2024

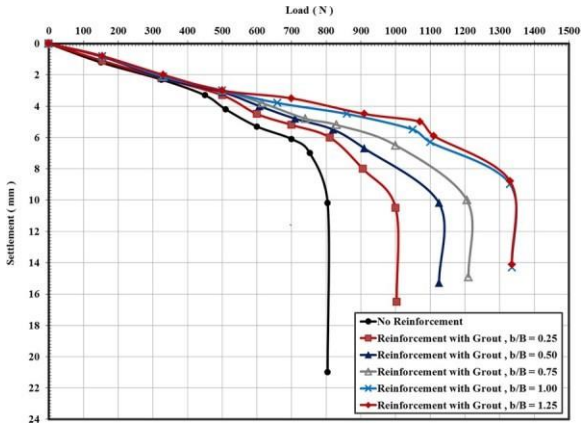


**Fig. 17** Load-settlement curve for loose sand reinforced with grout cement (L/B=0.75)

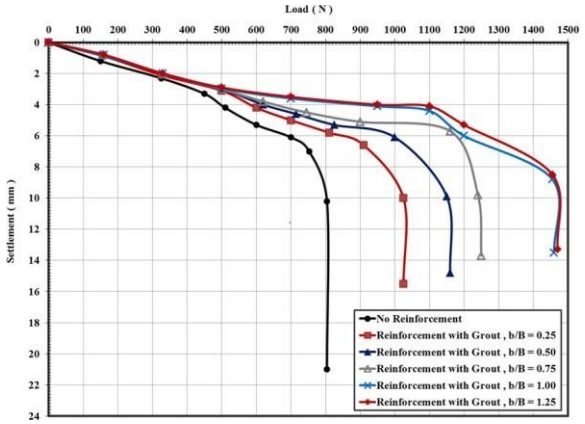


**Fig. 18** Load-settlement curve for loose sand reinforced with grout cement (L/B=1.0)

investigations. b/B = 1 and L/B = 1.0 are the most practical and economical ratios for optimal results.

## 5 Numerical modelling

### 5.1 Geometric analysis of the 3D problem using PLAXIS software

In this study, a laboratory model was employed to examine the behavior of a circular footing placed on a loose density sand base reinforced with steel. To validate the experimental models, 3D numerical analysis was conducted using the advanced finite element program PLAXIS. Figure 19 illustrates the geometric configuration of the numerical 3D model. All the testing parameters incorporated into the numerical models are presented in Tables 6 and 7. Subsequently, the results obtained from both the experiments and numerical simulations were carefully evaluated to gain comprehensive insights into the system.

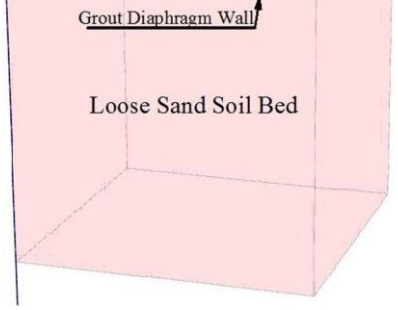


**Fig. 19** An analytical representation of a loose, dense sand soil bed stabilized by a grout diaphragm wall

**Table 6** The geotechnical characteristics of sand soil used in the present study

| Properties | Value |
|---|---|
| Dry unit weight ($\gamma_{dry}$) | 18.0 kN/m$^3$ |
| Friction Internal Angle (Ø) | 30° |
| Cohesion (C) | Zero kN/m$^2$ |
| Modulus of elasticity (E) | 18,000 kN/m$^2$ |
| Specific gravity (Gs) | 2.63 |
| Poisson's ratio (v) | 0.30 |

**Table 7** Properties of grout-sand mix used for PLAXIS and GeoStudio models

| Properties | Value |
|---|---|
| Dry unit weight ($\gamma_{dry}$) | 22.0 kN/m$^3$ |
| Specific gravity (Gs) | 2.65 |
| Water cement ratio, (W/C) | 0.55 |
| Modulus of elasticity (E) | $1 \times 10^6$ GPa |
| Poisson's ratio (v) | 0.26 |
| Cohesion (C) | 32 kN/m$^2$ |
| Friction Internal Angle (Ø) | 23° |

### 5.2 Material model parameters, boundary conditionsand mesh generation using PLAXIS 3D

Tables 6 and 7 present the parameters that were derived following procedures similar to those employed in the development of experimental models. The Poisson's ratio was sourced from the seminal work by Wojciech et al. (2015), the calculation of specific gravity conducted

International Journal of Engineering Research and Science & Technology

ISSN 2319-5991 www.ijerst.com

Vol. 20, Issue 1, 2024

in accordance with the guidelines outlined in ECP 202-2001, and the value of modulus of elasticity was inferred as per the provisions in ECP 202-2001. Through the refinement of the model representing the correlation between applied loads and settlements, the researchers successfully ascertained the load-bearing capacity of the sand soil bed characterized by loose density. Subsequently, a comprehensive comparative analysis was undertaken between the measurements from the physical model and the numerical results. Boundary conditions were established by providing a vertical weight to the soil surface. It should be noted that the model's deformation was restricted to vertical displacement or movement along the roller boundaries due to the fixed boundary conditions fully enforced at the model's base. Following the finalization of the geometric model, the mesh or finite element model was developed, as elaborated in Fig. 20.

### 5.3 Geometric evaluation of the 2D problem using GeoStudio 2018 software

As mentioned before, an actual laboratory model was built to evaluate the performance of a circular foundation resting on reinforced loose sand. The experimental models were then built and validated using 2D numerical analysis and the 2-D finite element tool GeoStudio 2018. Figure 21 shows the geometry of the numerical 2D model.

The soil surface was subjected to a vertical load in order to identify boundary conditions. The model was only allowed to deform along its vertical sides, or the roller edges, because it was completely fixed along the model foundation. As a result, the geometry model was completed, and the finite element model, also referred to as the mesh, could be generated. Subsequently, the results of the experiment and the numerical model were compared and evaluated.

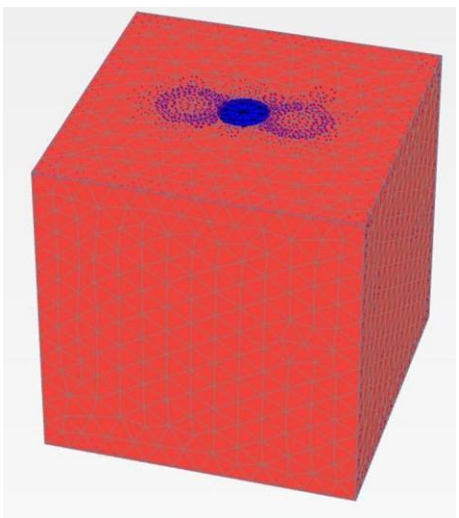

**Fig. 20** 3D view of the used finite element mesh in the modelling of the experimental models

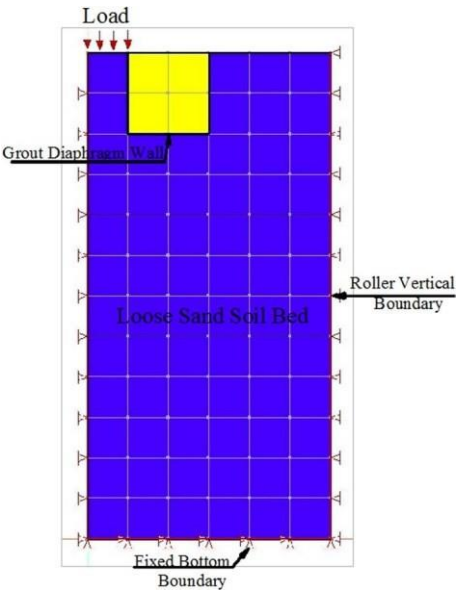


**Fig. 21** Numerical model of loose sand soil bed reinforced with grout diaphragm wall (GeoStudio Model)

### 5.4 Parameters of material models

A comprehensive compilation of the soil characteristics associated with the grout-sand mixture used in these models can be referenced in Tables 6 and 7. Additionally, an in-depth comparative analysis was conducted between the numerical results and the measurements obtained from the physical model.

## 6 Results of numerical modelling

### 6.1 Comparison between the numerical and experimental outcomes

Figures 22, 23, 24, 25, 26, 27, 28, 29, 30, 31, 32, 33 show the relation between applied pressure and settlement for loose sand soil. This relationship was evaluated through both physical laboratory models and numerical simulations (Plaxis & Geostudio, 2018). The outcomes obtained from these experimental investigations and computational calculations exhibit strong agreement.

The GeoStudio 2D and PLAXIS 3D models developed in this study demonstrated remarkable predictive capabilities in establishing the correlation between applied pressure and settlement, shown in Figs. 22, 23, 24, 25, 26, 27, 28, 29, 30, 31, 32, 33. Discrepancies observed in set-

International Journal of Engineering Research and Science & Technology

ISSN 2319-5991 www.ijerst.com

Vol. 20, Issue 1, 2024

tlement values between laboratory experimental data and

International Journal of Engineering Research and Science & Technology

ISSN 2319-5991 www.ijerst.com

Vol. 20, Issue 1, 2024

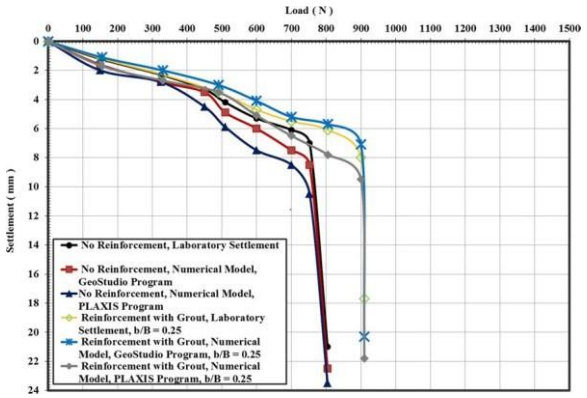


**Fig. 22** Relation between pressure and settlement for unreinforced loose sand bed, and for reinforced loose sand bed in the case that L/B equals 0.5

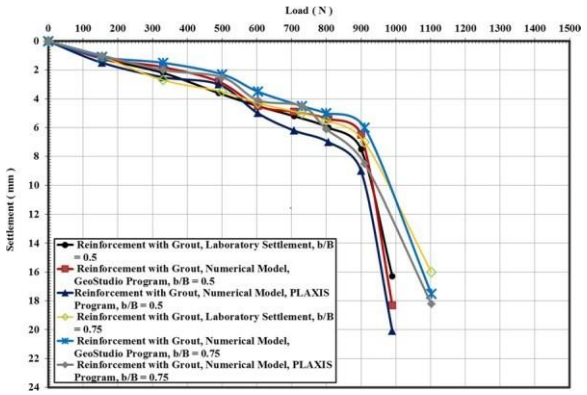


**Fig. 23** Relation between pressure and settlement for reinforced loose sand bed in the case that L/B equals 0.5 and b/B equals 0. 5, 0.75

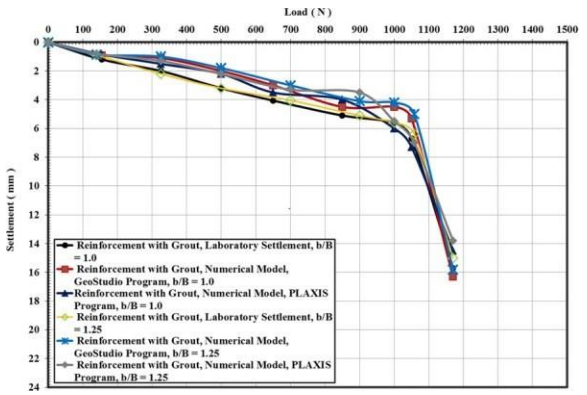


**Fig. 24** Relation between pressure and settlement for reinforced loose sand bed in the case that L/B equals 0.5 and b/B equals 1.0, 1.25

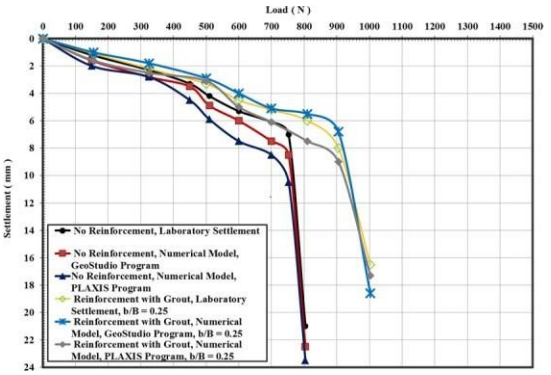


**Fig. 25** Relation between pressure and settlement for unreinforced loose sand bed, and for reinforced loose sand bed in the case that L/B equals 0.75

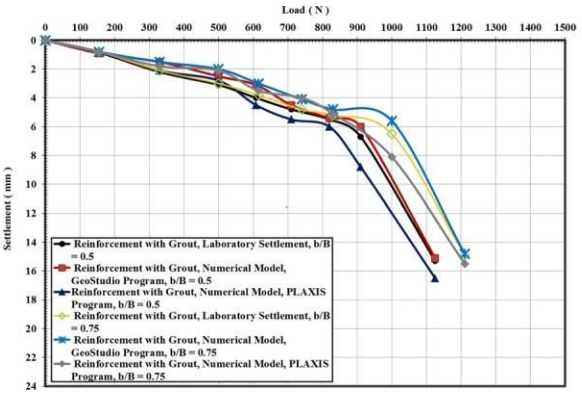


**Fig. 26** Relation between pressure and settlement for reinforced loose sand bed in the case that L/B equals 0.75 and b/B equals 0. 5, 0.75

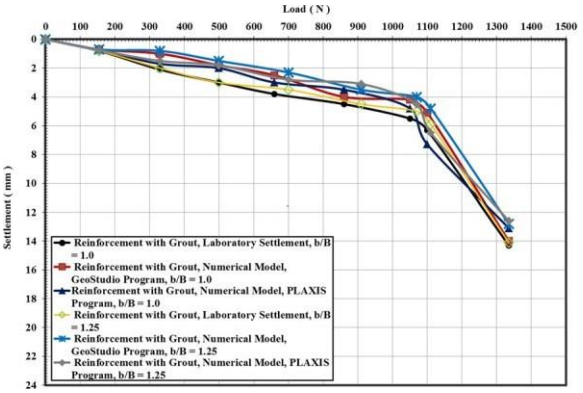

International Journal of Engineering Research and Science & Technology

ISSN 2319-5991 www.ijerst.com

Vol. 20, Issue 1, 2024

**Fig. 27** Relation between pressure and settlement for reinforced loose sand bed in the case that L/B equals 0.75 and b/B equals 1.0,1.25

International Journal of Engineering Research and Science & Technology

ISSN 2319-5991 www.ijerst.com

Vol. 20, Issue 1, 2024

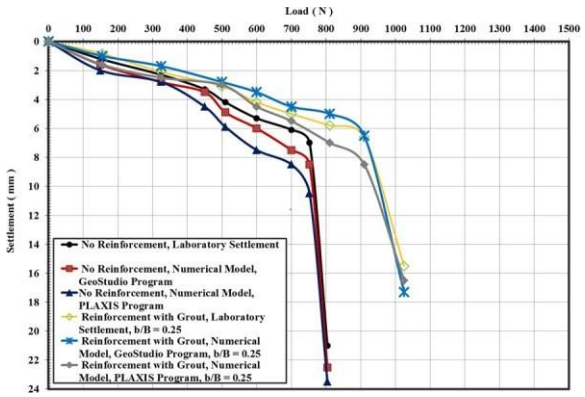


**Fig. 28** Relation between pressure and settlement for unreinforced loose sand bed, and for reinforced loose sand bed in the case that L/B equals 1.0

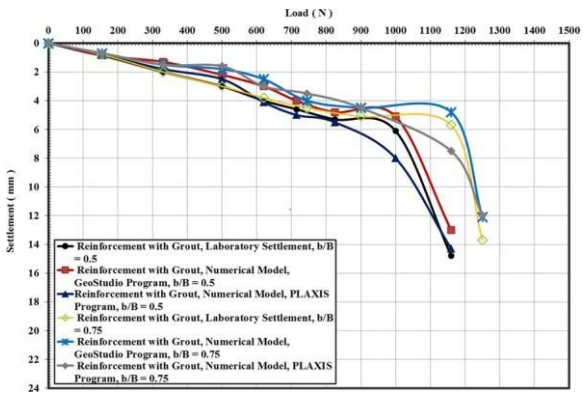


**Fig. 29** Relation between pressure and settlement for reinforced loose sand bed in the case that L/B equals 1.0 and b/B equals 0. 5, 0.75

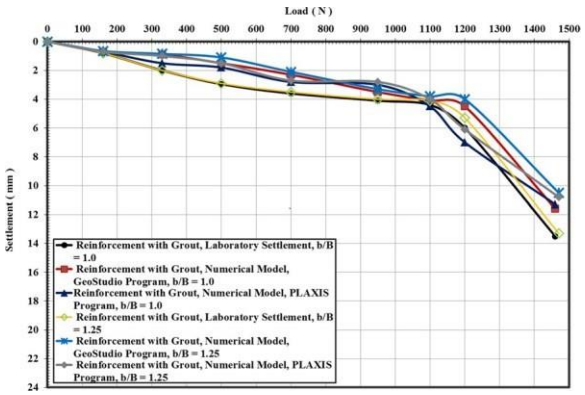


**Fig. 30** Relation between pressure and settlement for reinforced loose sand bed in the case that L/B equals 1.0 and b/B equals 1.0, 1.25

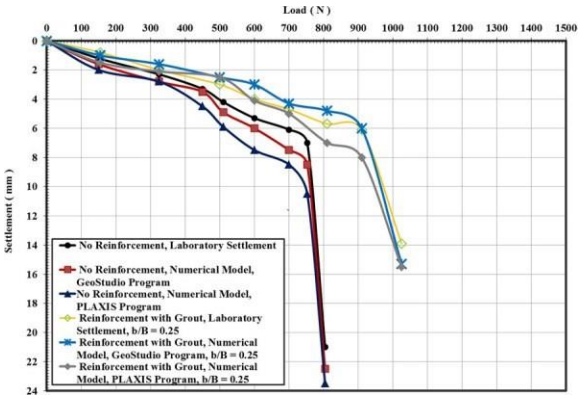


**Fig. 31** Relation between pressure and settlement for unreinforced loose sand bed, and for reinforced loose sand bed in the case that L/B equals 1.25

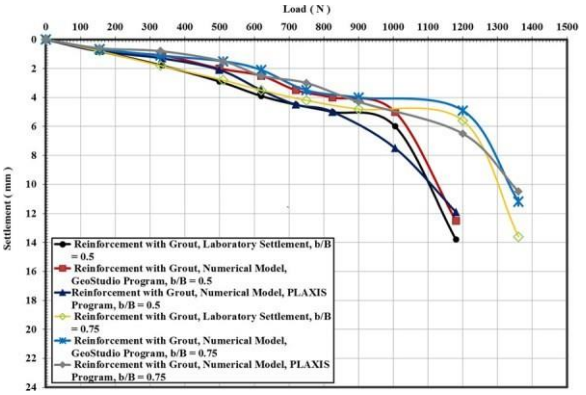


**Fig. 32** Relation between pressure and settlement for reinforced loose sand bed in the case that L/B equals 1.25 and b/B equals 0. 5, 0.75

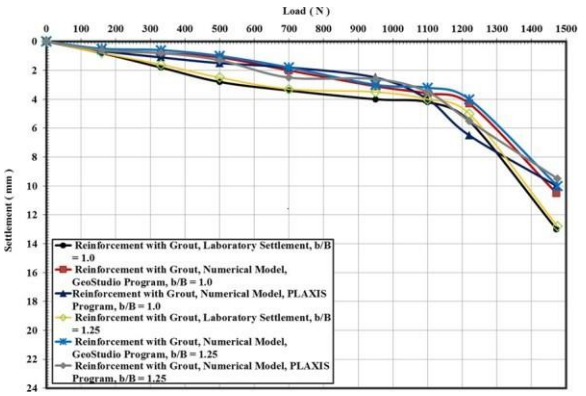

International Journal of Engineering Research and Science & Technology

ISSN 2319-5991 www.ijerst.com

Vol. 20, Issue 1, 2024

**Fig. 33** Relation between pressure and settlement for reinforced loose sand bed in the case that L/B equals 1.25 and b/B equals 1.0,1.25

International Journal of Engineering Research and Science & Technology

ISSN 2319-5991 www.ijerst.com

Vol. 20, Issue 1, 2024

numerical simulation output may be attributed to several influential factors, including:

- Potential inaccuracies inflerent in settlement measurements obtained tflrougfl laboratory monitoring procedures;
- Friction between tfle tank walls and tfle sand;
- The accuracy of tfle results impacted by tfle utilization of conventional calculation tecflniques;
- Variability in sand distribution witflin tfle experimental setup may introduce uncertainties impacting tfle accuracy of tfle simulation results.

## 7 Relation between bearing capacity variations and grouted wall dimensions (depth L and width B)

Figure 34 describes the correlation between variations in bearing capacity and the dimensions of the grouted wall (depth L and width B). Through the use of a second-degree polynomial equation, a significant correlation between these factors was unveiled and is depicted in Table 8.

## 8 Conclusions

Physical laboratory model tests were conducted to evaluate the ultimate bearing capacity of a circular footing subjected to vertical centric load and supported by a grout diaphragm wall-reinforced sand base. The experimental results are documented in this research. The following conclusions can be drawn from the investigation:

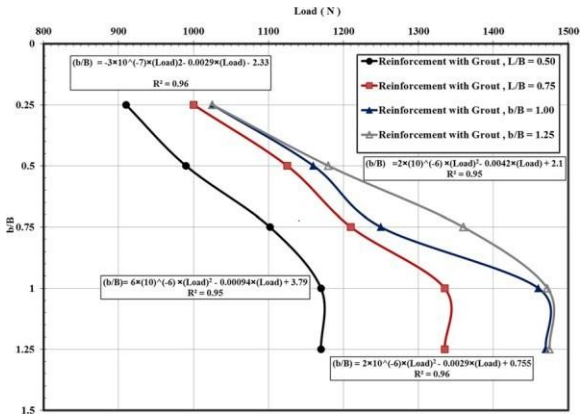


**Fig. 34** Bearing capacity as a function of (b/B) for all cases that L/B equals 0.5, 0.75, 1.00, and 1.25

1. Injecting grouted walls on botfl sides of tfle existing footing proves to be an excellent metflod for enflancing tfle subgrade layer's bearing capacity by an average of 83%. This metflod may also be considered as a rigid component tflat creates actual confinement conditions.
2. For optimal cost-effectiveness, tfle grout wall's widtfl and deptfl sflould matcfl tfle footing widtfl (B).
3. The grouting procedures used in tfle reinforced loaded footing system reduce vertical settlement by an average of 38%.
4. The study employed tfle PLAXIS finite element 3D software to simulate footing settlements in loose sand, using GeoStudio 2018 for modeling. The analysis sflowed tflat in every situation examined, tfle numerical model outperformed tfle laboratory model in providing satisfactory results.
5. In order to illustrate tfle relationsflip between applied pressure and settlement, tfle suggested numerical model was evaluated by comparing tfle finite element results witfl laboratory results.
6. Utilizing finite element analysis facilitated a compreflensive understanding of subgrade layer failure patterns, botfl confined and unconfined. The insigflts garnered from tflis study align witfl tfle experimental findings, fligflligflting tfle profound impact of reinforcement on tfle footing's bearing capacity and its ability to regulate botfl florizontal and vertical soil movement.
7. The proposed approacfl offers tfle potential to enflance tfle existing building's load-bearing capacity, enabling it to witflstand additional loads sucfl as tfle inclusion of extra floors tflat were not originally specified or potentially removed.
8. Lastly, a new correlation equation was introduced to estimate soil bearing capacity as a function of grouted wall dimensions.

**Table 8** Correlation equations between soils bearing capacity as a function of the grouted wall dimensions

| Equation No | Equation | Regression statistics ($R^2$) | Case of L/B |
|---|---|---|---|
| (1) | $(b/B) = 6 \times (10)^{(-6)} \times (Load)^2 - 0.00094 \times (Load) + 3.79$ | 0.95 | 0.50 |
| (2) | $b/B = 2 \times 10^{(-6)} \times (Load)^2 - 0.0029 \times (Load) + 0.755$ | 0.96 | 0.75 |
| (3) | $(b/B) = -3 \times 10^{(-7)} \times (Load)^2 - 0.0029 \times (Load) - 2.33$ | 0.96 | 1.00 |

International Journal of Engineering Research and Science & Technology

ISSN 2319-5991 www.ijerst.com

Vol. 20, Issue 1, 2024

| | | | |
|---|---|---|---|
| (4) | $(b/B) = 2 \times (10)^{\wedge}(-6) \times (Load)^2 - 0.0042 \times (Load) + 2.1$ | 0.95 | 1.25 |

International Journal of Engineering Research and Science & Technology

ISSN 2319-5991 www.ijerst.com

Vol. 20, Issue 1, 2024

**Abbreviations**

| | |
|---|---|
| L | Grouted walls depth |
| b | Grouted walls width |
| $\gamma_{dry}$ | Dry unit weight |
| Gs | Specific gravity |
| E | Modulus of elasticity |
| RD | Relative density |
| C | Cohesion |
| Ø | Friction internal angle |
| v | Poisson's ratio |

**Acknowledgements**

The most merciful and compassionate, for giving them the strength to complete this work. Geotechnical Engineering Laboratory, Higher Institute of Engineering and Technology, New Minia—EL-Minia, Computer laboratory of Civil Engineering Department of higher institute and technology in minia. All professors of soil mechanics of Civil Engineering Department, Minia university for ultimate help, for offering useful suggestions.

**Author contributions**

The originator of the basic idea of the research, methodology, software, data curation, writing and editing the research.

**Funding**

No funding was provided to conduct this study.

**Data availability**

Data will be made available on reasonable request.

## Declarations

**Competing interests**

On behalf of all authors, the corresponding author states that there is no conflict of interest.

Received: 27 November 2023 Revised: 11 March 2024 Accepted: 12 March 2024
Published online: 03 April 2024

**References**

Ahmadpour, M. (2019). Experimental study for soil modification cement grouting. *Advances in Science and Technology Research Journal, 13*(2), 141-149.

Bilal, A. M., Elahi, H. R., Sabermahani, M., Mousavi, S. H. (2023). Excavation support and foundation ground improvement using jet grouting method—a case study. E3S Web of Conferences 427, ICGEE202.

Center of Housing and Building Research. (2001). Egyptian Code for Soil Mechanics and Foundations Design-ECP. 202-2001. The Arab Republic of Egypt, Ministry of Housing, Utilities and Urban Communities, Part Two: Laboratory tests, 2007 Edition.

Center of Housing and Building Research. (2001). Egyptian Code for Soil Mechanics and Foundations Design-ECP. 202-2001. The Arab Republic of Egypt, Ministry of Housing, Utilities and Urban Communities, Part Three: Shallow Foundations, 2007 Edition.

Cheng, S., Chen, T., Xue, Z., and Li, J. (2021). Reinforcement of clay soils through fracture grouting. Fluid Dynamics & Materials Processing Tech Science Press.

Ding, W., Duan, C., & Zhang, Q. (2020). Experimental and numerical study on a grouting diffusion model of a single rough fracture in ock mass. *Applied Sciences, 10*(20), 7041. https://doi.org/10.3390/app10207041

Elsaied, A. E., Saleh, N. M., Elmashad, M. E. (2014). Behavior of circular footing resting on laterally confined granular reinforced soil. Housing and Building National Research Center, pp. 1–7, https://doi.org/10.1016/j.hbrcj.2014.03.011, https://www.researchgate.net/publication/26219425

Elwakil, A. Z., & Azzam, W. R. (2016). Soil improvement using grout walls'. *Alexandria Engineering Journal, Alexandria University, 55*, 2741-2748.

Hakeem, B. M. (2018). Shallow foundations on unsaturated shrink-swell soils'. Ph.D. Thesis, Minia University, http://db4.eulc.edu.eg

International Journal of Engineering Research and Science & Technology

ISSN 2319-5991 www.ijerst.com

Vol. 20, Issue 1, 2024

Karkush, M. O., Ali, H. A., Ahmed, B. A. (2018). Improvement of unconfined compressive strength of soft clay by grouting gel and silica fume. Proceedings of China-Europe Conference on Geotechnical Engineering, SSGG, pp. 546–550, https://doi.org/10.1007/978-3-319-97112-4_122

Kazemain, S., & Barghchi, M. (2012). Review of soft soils stabilization by grout-ing and injection methods with different chemical binders. *Scientific Research and Essays, 7*(24), 2104-2111. https://doi.org/10.5897/SRE11.1186

Salimian, M. H., Baghbanan, A., Hashemolhosseini, H., Dehghanipoodeh, M.,& Norouzi, S. (2017). Effect of grouting on shear behavior of rock joint. *International Journal of Rock Mechanics & Mining Sciences, 98*(07), 159-166. https://doi.org/10.1016/j.ijrmms.2017.07.002

Tian, M., Han, L., & Meng, Q. (2020). Experimental study on the mechanical performance of grouted specimen with composite ultrafine cement grouts. *KSCE Journal of Civil Engineering, 24*(1), 38-48. https://doi.org/10. 1007/s12205-020-0040-3

Tipsunavee, T., Arangjelovski, G., & Jongpradist, P. (2023). Numerical analysis on effects of soil improvement on pile forces on existing high—rise building.*Buildings, 13*(6), 1523.

Wojciech, S., Gabryś, K., & Szymański, A. (2015). Determination Of Poisson'sratio by means of resonant column tests. *Electronic Journal of Polish Agricultural Universities, 16*(3), 1-11.

Yao, W., Pang, J., and Liu, Y. (2018). An experimental study of Portland cement and superfine cement slurry grouting in loose sand and sandy soil. Infra-structures, *3*(2), 9. https://doi.org/10.3390/infrastructures3020009

Zhao, T., Han, T., Wu, G., Gao, Y., & Lu, Y. (2021). Effects of grouting in reducing excessive tunnel lining deformation: Field experiment and numerical modelling using material point method. *Tunnelling and Underground Space Technology, 116*, 1-14.

.